Demonstrating real-time hydrodynamic motion response in force control for regular waves in a robotized dry test rig with a point-absorber WEC

Dana Salar, Erik Hultman

Abstract— **A 6-Degrees-Of-Freedom robotized dry test rig has been developed at Uppsala University to test point absorbing WECs (Wave Energy Converters). Using a six joint industrial robot as a buoy movement emulator, the robot's outermost point (joint 6) is connected to the wire from the generator concept WEC PTO (Power Take-Off). The robot's movement in joint 6 thus corresponds to the buoy movement on the sea surface. The test rig can be used for various point absorbing WEC PTO units. In this project, the test rig has been used with a WEC-PTO prototype. The point absorbing WEC-LRTC concept is being developed at Uppsala University. The generator concept is made up of two identical rotating generators. A wire is used as a connection between the generator concept at the seabed and a buoy on the sea surface.**

The goal of this article is to demonstrate and evaluate how the test rig interacts with the LRTC-WEC PTO in regular waves. In the presented experiments, a hydrodynamic model with force control method has been used.

The results show a clear difference in the use of the hydrodynamic model with different sizes of the buoy. The test rig with the force control model can be used easily to test different theoretical buoys and different load settings for WEC PTOs. Effective experiments can be performed with real PTO forces instead of simplified simulations.

Future work is to experiment with the position control method and also experiments with irregular waves.

Keywords— dry test rig, industrial robot, LRTC, point-absorber, wave emulator, wave energy converter

I.INTRODUCTION

The need for renewable energy in the world is increasing and the demand for environmentally friendly electrical energy, green energy is increasing. Ocean waves are an attractive source of energy for many researchers around the world [1]. There are a few point absorbing WECs (Wave Energy Converters) that have already been developed worldwide. Research is ongoing around the world for the development of more efficient and sustainable WECs that also have to be economically rewarding [2][3][4].

For more than 20 years, Uppsala University has begun to focus on renewable energy production. At Uppsala University, different types of renewable energy sources have been evaluated including several WECs [5]. One of them is the LRTC (Low Rpm Torque Converter) concept [6][7]. The concept is made up of two rotating generators, the generators placed against each other. The rotating shaft of the generators are connected to each other via a drum. Two clutches and a spring are implemented in the drum. The clutches allow each generator to spin only in one direction (opposite to each other). A wire is spun around the drum and connected to a buoy on the sea surface. With the movement of the waves, the buoy gets up which pulls around generator 1 and the buoy on the way down pulls the spring around generator 2 (see Fig.1).

All kinds of WECs have to be tested in some way with a PTO (Power Take-Off) and validated during the entire development phase. Limitations of test environments and its costly methods have slowed down the development of WECs. Today, the WEC concepts are tested in different ways, there is tests directly in open sea, which is difficult and time-consuming, and there are also experiments in wave tanks and on shore dry test rigs [8][9][10][11]. The advantage of the robotized dry test rig used in this article compared to other dry test rigs is that it is flexible, can work in 6-DOF and is an industrial general machine concept.

At Uppsala University, a dry test rig with a six-jointed 6-DOF (Degree Of Freedom) industrial robot has been developed to test and validate WEC concepts on a smaller scale (see Fig.2).

In the past, the robot has been used as a test rig to passively test and validate the performance of the LRTC-WEC concept [6][7]. The test rig has since then been further developed with the implementation of a hydrodynamic model [12].

The purpose of this article is to demonstrate and evaluate the interaction of the dry test rig including the

D. S. Author is with the Department of Electrical Engineering at Uppsala University, Box 65, 75103 Uppsala, Sweden (dana.salar@angstrom.uu.se).

E. H. Author is with the Department of Electrical Engineering at Uppsala University, Box 65, 75103 Uppsala, Sweden (erik.hultman@angstrom.uu.se).

Digital Object Identifier: https://doi.org/10.36688/ewtec-2023-643

hydrodynamic model with a PTO. In this article, the test rig is used with the LRTC-WEC PTO in only vertical direction (heave) using a force control method in the robot system.

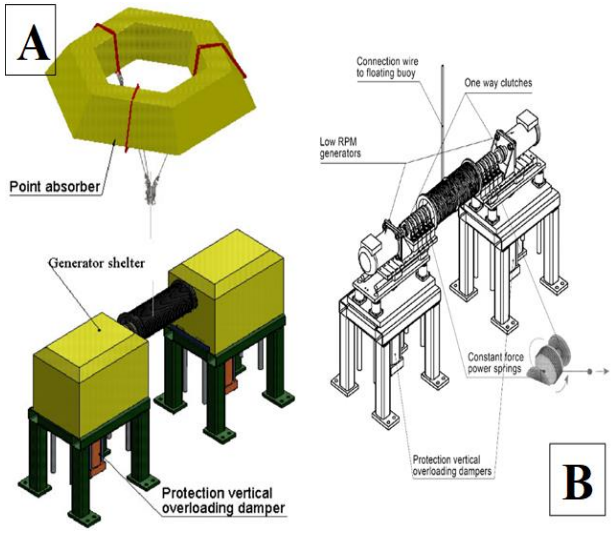

Fig. 1. LRTC-WEC concept

II.METHOD

In this article, various methods have been used including both experiments and theoretically calculations.

1) *Experiment setup*

An industrial 6-DOF robot of the model IRB6650S, manufactured by ABB, payload of 200 kg, a range of 3 m and position repeatability 0,14 mm is used in the robotized dry test rig.

The robot is used to emulate the buoy motion in the sea waves. The wire from the LRTC-PTO, which in reality is connected to a buoy on sea surface, is in this experiment connected to the robot's outermost joint (joint 6) (see Fig.2).

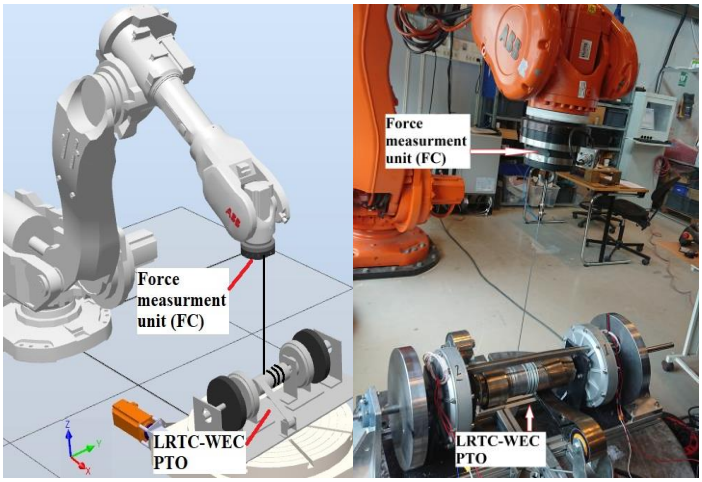

Fig. 2. The robotized dry test rig with the LRTC-WEC PTO

In this dry test rig system, the robot is equipped with an ABB FC (Force Controller) 6-DOF force measurement unit and a software for FC. A hydrodynamic motion model is implemented directly in the robot controller, processed by the robot control system. A waveform is sent to the robot control system, the robot will act as a buoy on the sea surface. In this article we investigate the force control method from [12] but with 500 N/(m/s) force sensitivity.

The LRTC PTO system used in this article is from [7].

2) *Hydrodynamic model*

In order for the robot to behave like a buoy in real time, a hydrodynamic model was implemented in the test rig. The emulated hydrodynamic response is affected by the size and the shape of the buoy, the incoming wave and the mechanical PTO force from the LRTC-WEC.

The hydrodynamic model calculation is divided into three main parameters, hydrodynamic force from the buoy F_{hyd}, acceleration force from the buoy F_{buoy} and the mechanical forces from the LRTC-WEC, F_{mec} (see Fig.4) [13][14][15]. In this case F_{mec} includes both the mechanical and the damping PTO forces.

$$F_{buoy} = F_{mec} + F_{hyd} \tag{1}$$

F_{mec} is measured with the FC unit while F_{hyd} and F_{buoy} are calculated every 24 ms in the robot controller. From this reference a force F_{ref} is calculated and set to the robot force controller:

$$F_{ref} = F_{hyd} + F_{buoy} - F_{standstill} \tag{2}$$

Where $F_{standstill}$ is the standstill force from the LRTC-PTO (constant force spring). For a buoy in real operation, there should be an equilibrium between all forces. Since F_{mec} is measured by the FC sensor, the robot will thus strive to move so that F_{ref} cancel out F_{mec} and hence a buoy motion is emulated (see Fig. 3). To implement this hydrodynamic model, the buoy acceleration and velocity are derived from the buoy (robot) position and low-pass

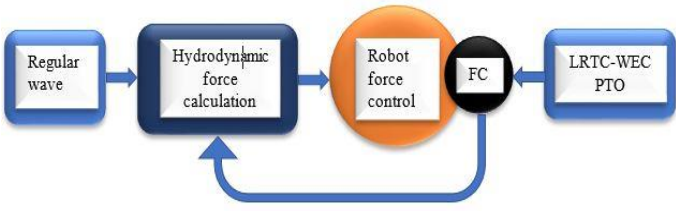

Fig. 3. The hydrodynamic force control model use in the test rig

filtered. F_{buoy} is then calculated based on Newton's second law, in this case we have the buoy mass m and the buoy acceleration is $\ddot{x}(t)$:

$$F_{buoy} = m\ddot{x}(t) \tag{3}$$

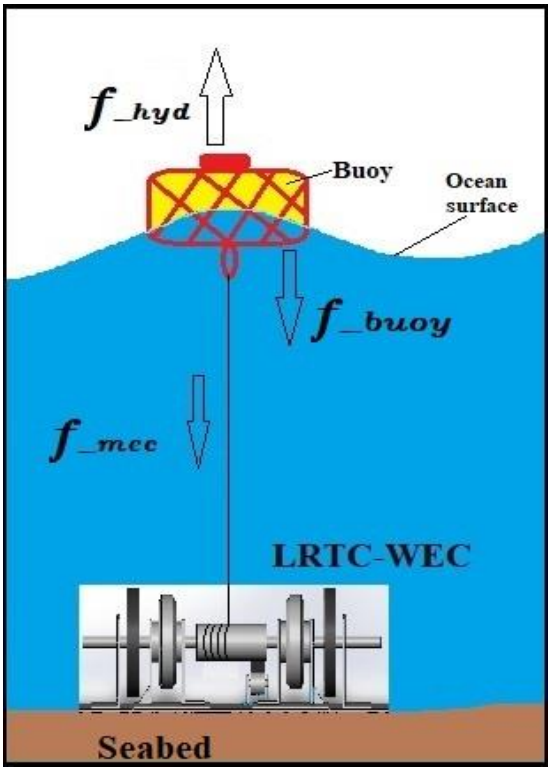

Fig. 4. Hydrodynamic forces

The hydrodynamic force is calculated relative the buoy equilibrium position and consist of the excitation force F_e, the hydrostatic force F_{hs} and the radiation force F_r which calculated based on the wave motion [13]:

$$F_{hyd} = F_{hs} + F_r + F_e \tag{4}$$

$$F_{hs} = \rho g A_s x(t) \tag{5}$$

$$F_r = A_m(\omega)\ddot{x}(t) + B_c(\omega)\dot{x}(t) \tag{6}$$

Where ρ is the liquid density, g is the acceleration of gravity, A_s describes the transverse area of the buoy, x(t) is the vertical displacement of the buoy, A_m is the added mass, B_c is the damping coefficient, ω is the wave angular frequency and $\dot{x}(t)$ is the buoy velocity.

The excitation force for regular wave as we use in this project is:

$$F_e = \Gamma(\omega)\frac{H_S}{2} sin\omega t \tag{7}$$

Where Γ(ω) is the force amplitude and H_s is the significant wave height:

$$\Gamma(\omega) = \sqrt{\frac{2g^3\rho B_c(\omega)}{\omega^3}} \tag{8}$$

TABLE 1 BUOY PARAMETERS

	D (m)	h (m)	m (kg)	A_m (kg)	B_c (Ns/m)
Buoy 1	1.2	0.5	100	550	180
Buoy 2	0.6	0.5	25	64	12

3) Simulation experiment set

The buoy motion was also simulated in Simulink, using the same force model and with 10 ms time-step size. A simplified LRTC-PTO force model was here used to simulate F_{mec} as being proportional to the buoy velocity using the LRTC damping factor D_{mec} set to -500 N/(m/s). Since the model is based on the buoy equilibrium position, the LRTC-PTO constant force springs could be neglected in the simulation. The robot damping sensitivity force F_{rob} was simulated the same way as the F_{mec}, setting the robot damping factor D_{rob} to -500 N/(m/s). After calculating F_{buoy} using Eq. 1 but now also adding F_{rob}, Eq. 3 was used to calculate the buoy acceleration. Finally, a continuous integrator function was used to calculate the buoy velocity and position. A conceptual illustration of the Simulink model is shown in Fig. 5.

4) Experiments

In this project we only experimented with regular waveform, sinus wave in vertical direction (heave). Due to limitations in the ABB force control application, we have not been able emulate higher wave velocities. The tests were made only with sine waves in heave direction, the simulation coefficients are based on a specific buoy size. In this test, two different cylindrical buoys with diameter *D*, height *h* and mass *m* were used (see Table 1). The software WAMIT was used to obtain buoy parameters A_m and B_c constants used in the calculations.

Three different experiments were performed with the same regular wave sample:

I. A sine wave with an amplitude of 200 mm and a period of 4 s during five full periods

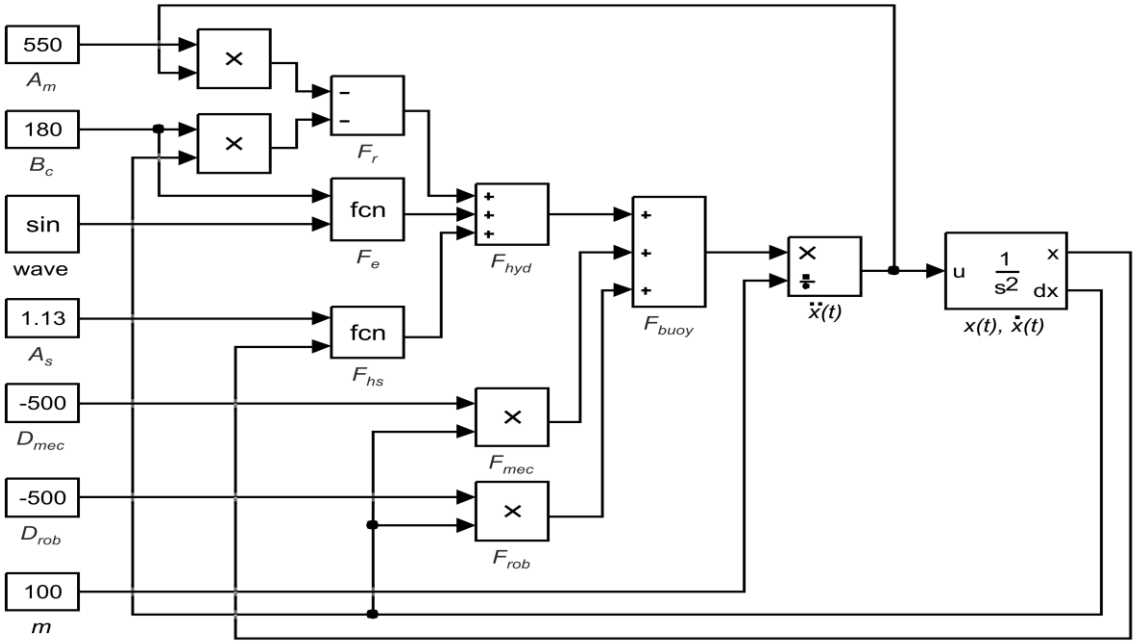

Fig. 5. Simulink simulation of the hydrodynamic model used in the test rig

Experiment one (Exp.1) were done without the effect of the hydrodynamic forces with the LRTC-WEC electrically loaded. For this experiment the buoy size or the PTO forces does not matter as the robot movement will be identical to the wave movement.

Exp.1.i Sine wave, LRTC loaded

Experiment two (Exp.2) was done with the hydrodynamic force model and the LRTC-WEC electrically loaded and unloaded for both of buoy 1 and buoy 2:

Exp.2.i Buoy 1, LRTC loaded

Exp.2.ii Buoy 1, LRTC unloaded

Exp.2.iii Buoy 2, LRTC loaded

Exp.2.iv Buoy 2, LRTC unloaded

Experiment three (Exp.3) is a simulation model of the buoy movement with the hydrodynamic force model made in the software MATLAB-Simulink (see Fig 5):

Exp.3.i Buoy 1, simulation model LRTC loaded

Exp.3.ii Buoy 2, simulation model LRTC loaded

III.RESULTS

In Fig. 6 results from Exp.1 and exp.2 show how the movement of the various buoys looks compared to the sine wave used in this case Exp.1.i. Table 2 and Fig.7 present the power output between Exp.1 and Exp.2.

Fig. 8 results from the simulation experiment show two different buoy movements which are compared with both the incoming wave and with the result from Exp.2.

TABLE 2 PEAK AND AVERAGE POWER OUTPUT RESULTS EXP.1 (TEST RIG WAVE MOTION) AND EXP.2(TEST RIG BUOY EMULATION)

	Generator 1 Output Peak Power (W)	**Generator 2 Output Peak Power (W)**	**Generator 1 Output Average Power (W)**	**Generator 2 Output Average Power (W)**	**LRTC Average Power comparison (%)**
Exp.1.i	11.7	11.6	3.0	3.0	100
Exp.2.i	11.0	10.8	2.8	2.6	90
Exp.2.iii	6.3	5.5	1.6	1.4	50

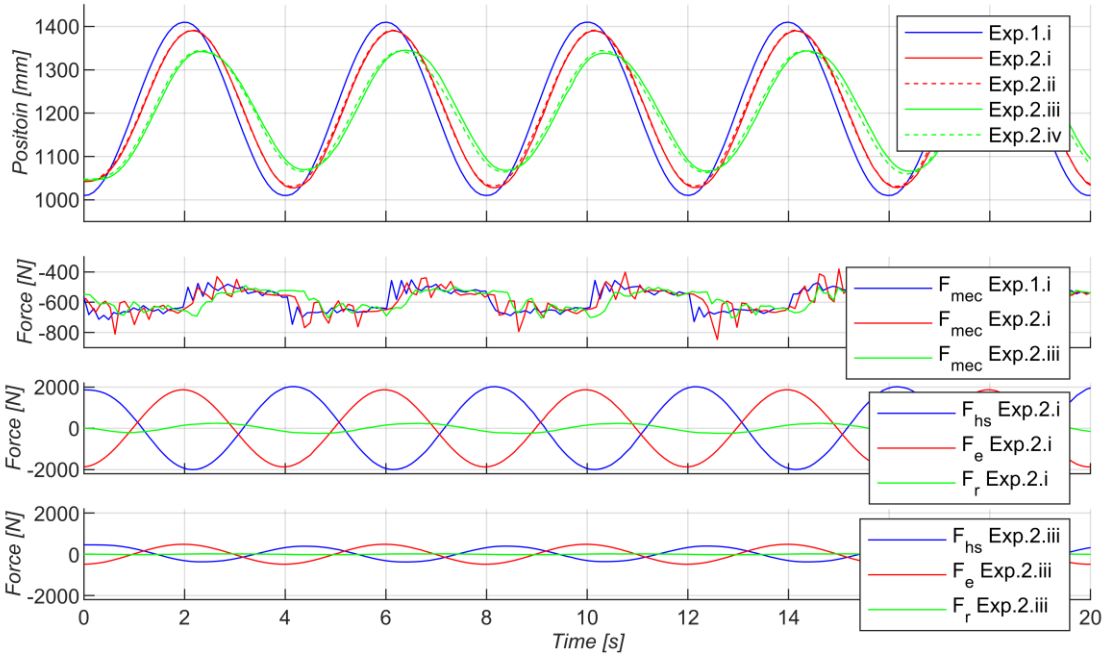

Fig. 6. Position and force results for Exp.1 (test rig wave motion) and Exp.2 (test rig buoy emulation)

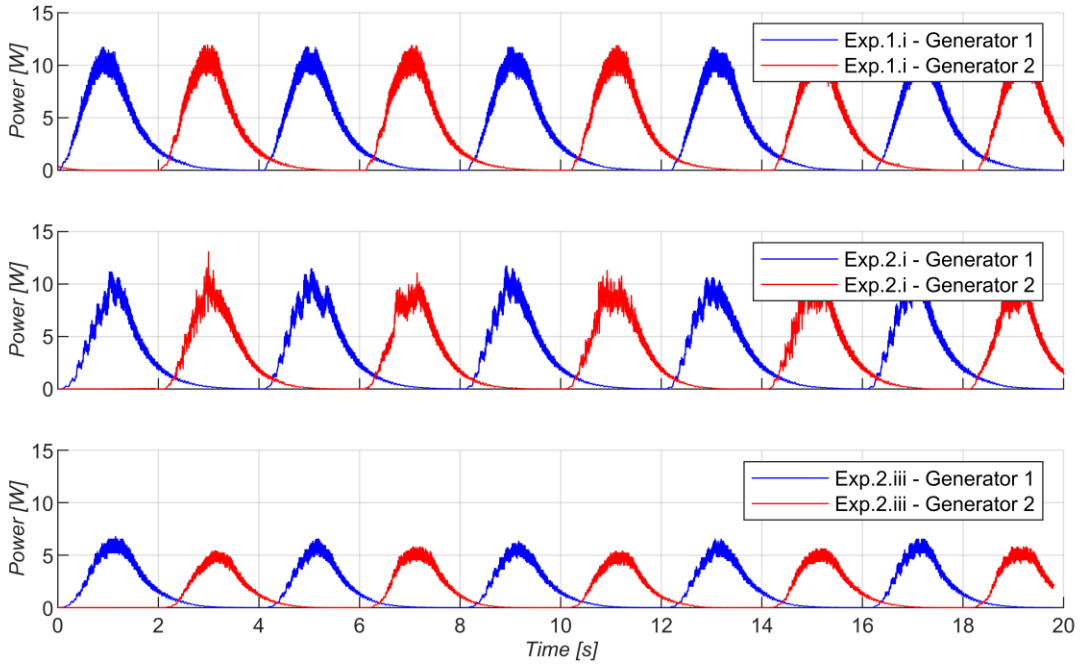

Fig. 7. Power output for Exp.1 (test rig wave motion) and Exp.2 (test rig buoy emulation)

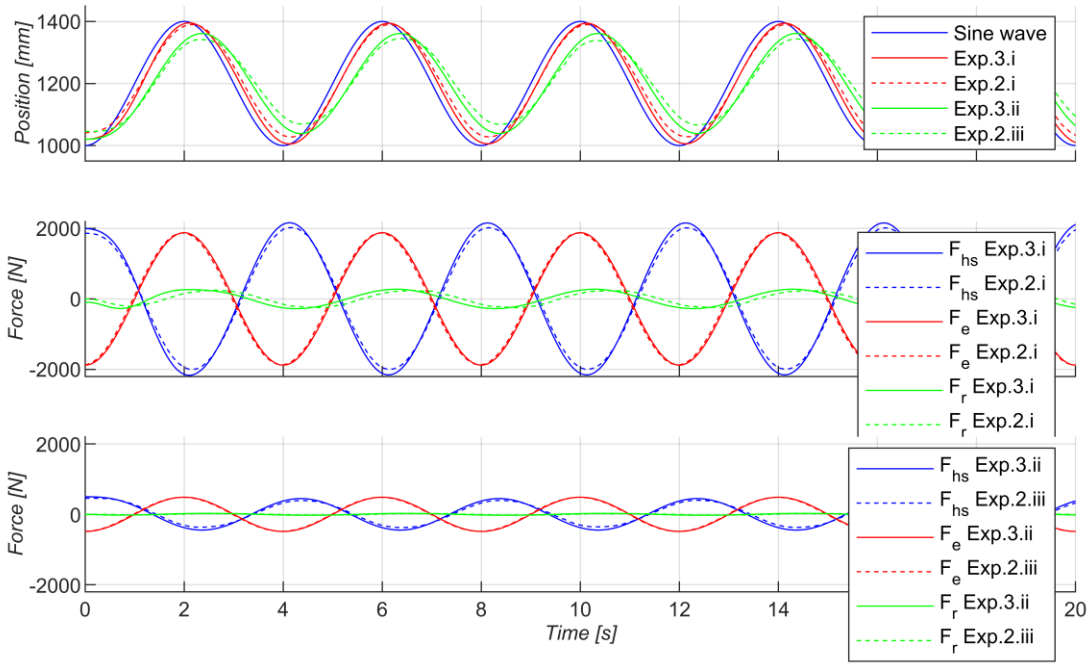

Fig.8. Position and force result for Exp.3 (buoy simulation) compared to Exp.2 (test rig buoy emulation)

IV.DISCUSSION

In Fig. 6 it can be seen that we can simulate the movement of different buoys. The result from Exp.2 (see Fig. 6) shows the motion difference between two buoy sizes with the influence of the hydrodynamic forces and the sine wave used. The Exp.2.i curve deviates less from the wave than Exp.2.iii because the buoy in Exp.2.i is larger than the buoy in Exp.2.iii and is more affected by those hydrodynamic forces. From the figure it can also be seen a small difference in the curves between when the LRTC is electrically loaded or unloaded. In Exp.2.iii the movement is more damper by the LRTC PTO because the buoy is smaller in size compared to the buoy in Exp.2.i.

It can be seen the power output in table 2 and in Fig.7. Generator 1 is pulled around while the robot is going up and generator 2 is pulled around with spring force while the robot is going down. That the power curve goes down more smoothly depends on the flywheels that are connected to the generators.

In table 2 we clearly see the differences in power output between Exp.1 and Exp.2 down to 50% less power output depending on buoy size. Peak power output in Exp.1 is more than Exp.2 is due to the movement is larger in amplitude, in this case also the average power is higher. The difference in power output between Exp.2i and Exp.2.iii depends on the size of the buoy, where in Exp.2.i is larger than in Exp.2.iii and therefore achieve higher movement in amplitude and also higher peak and average power output. In Exp.2.i, the power curve looks spiky and more uneven compared to Exp.2.iii may be due to the robot's FC was set to high sensitivity in combination with high reference force.

Exp.3 shows that the result in general the simulations agree well with the experiments in Exp.2. In Fig.8 we see the lag in the force F_r for Exp.2 compared to Exp.3, this is because speed and acceleration are derived from the robot's position and then low-pass filtered to obtain even values, so speeds and accelerations are obtained with a certain delay, which in turn affects the calculated value of F_r. The force F_e is not affected by the motion of the buoy and that is why the results from Exp.2 and Exp.3 clearly overlap.

The noticeable difference in movement between experiment results and simulation results because the LRTC simulation model is not identical to the LRTC concept, the model is roughly estimated. It is difficult to estimate all possible forces from the LRTC or other WEC concept. Other potential resonance for deviations between the simulation and the robotized experiments are the hydrodynamic model is executed with position control instead of force control in the simulation, that smaller time-steps are used in the simulation and that there might be limitations in the robot FC application.

We have not been able to validate the test rig with the implemented hydrodynamic model fully. A more accurate simulation model of a WEC concept needs to be developed or a practical experiment in a wave tank can be performed to be able to compare the result with the test rig system for validation of the test rig system including the hydrodynamic model.

Finally, it should be noticed that the robot damping force dose not in real off-shore operation.

1) Future work

A more accurate simulated LRTC model should be developed for more accurate comparison and to be able to validate the test rig system. Also, similar experiments as in

this article but with the position control method instead of force control are interesting.

V.CONCLUSIONS

The experiments with the robotized dry test rig connected to a PTO system have shown positive results regarding the interaction of the test rig with a PTO system. From the experiments and results obtained in this article, the aim of the article has been achieved.

The results show that the test rig in force control mode can be used easily to test different theoretical buoys and different load settings for WEC PTOs. Effective experiments can thereby be performed with real PTO forces instead of simplified simulations.

ACKNOWLEDGEMENTS

The authors are grateful to ABB Corporate Research, for the donation of the robot used in the experiments. ABB Robotics is acknowledged for providing the Force Control system used in the experiments. The Swedish STandUP for Energy research alliance, a collaboration initiative financed by the Swedish government, is acknowledged for contributing to the research infrastructure. The authors are thankful to Antoine Dupuis for generating hydrodynamic buoy parameters for the experiments.

VI.REFERENCES

[1] Junejo F, Saeed A and Hameed S (2018) Energy Management in Ocean Energy Systems. Comprehensive Energy Systems, VOL.5, pp 778-807, https://doi.org/10.1016/B978-0-12-809597-3.00539-3.

[2] Mueller M. and Wallace R (2008), Enabling science and technology for marine renewable energy, EnergyPolicy, vol. 36, no. 12, pp. 4376-4382

[3] Elwood D, C. Yim S, Prudell J, Stillinger C, von Jouanne A, Brekken T, Brown A, and Paasch R (2010) Design, construction, and ocean testing of a taut-moored dual-body wave energy converter with a linear generator power take-off. Renewable Energy, Volume 35, pp.348−354.

[4] Dongsheng Q, Rizwan H, Jun Y, Dezhi N and Binbin L (2020) Review of Wave Energy Converter and Design of Mooring System. Sustainability, 12(19), 8251.

[5] Leijon M, Boström C, Danielsson D, Gustafsson S, Haikonen K, Langhamer O, Stromstedt E, Stålberg M, Sundberg J, Svensson O, Tyrberg S, and Waters R (2008) Wave energy from the North Sea: Experiences from the Lysekil research site. Surveys in Geophysics, Volume 29, pp.221−240.

[6] Savin A, Salar D and Hultman E (2021) Low-RPM Torque Converter (LRTC). Energies, VOLUME 14, NO. 16, ARTICLE NUMBER 5071.

[7] Salar, D., Hultman, E. and Savin, A. (2023). The Low-RPM torque converter (LRTC) with Integrated direct shaft flywheel. *International Marine Energy Journal*, *6*(1), 1–10. https://doi.org/10.36688/imej.6.1-10

[8] Falcão, A.F.O. Henriques, J.C.C. Model-prototype similarity of oscillating-water-column wave energy converters. *Int J of Marine Energy* **2014**, *6*, 18-34. http://dx.doi.org/10.1016/j.ijome.2014.05.002

[9] Bracco, G., Giorcelli, E., Mattiazzo, G., Orlando, V. and Raffero, M. Hardware-in-the-loop test rig for the ISWEC wave energy system. *Mechatronics* **2015**, *25*, 11-17. http://dx.doi.org/10.1016/j.mechatronics.2014.10.007

[10] Bacelli, G., Spencer, S.J., Patterson, D.C., Coe, R.G. Wave tank and bench-top control testing of a wave energy converter. *Applied Ocean Research* **2019**, *86*, 351-366.

[11] Eriksson M, Waters R, Svensson O, Isberg J and Leijon M (2007) Wave power absorption: Experiments in open sea and simulation. J. Appl. Phys., vol. 102. https://doi.org/10.1016/j.apor.2018.09.009

[12] Hultman E and Salar D (2023) A robotized 6-DOF dry test rig for wave power. Sustainable Energy Technologies and Assessments, Volume 59, 103393, https://doi.org/10.1016/j.seta.2023.103393

[13] Iván A. Hernández-Robles, Xiomara González-Ramírez, Julián A. Gómez-Gutiérrez and Juan M. Ramirez (2021) Wave power assessment for electricity generation with powerbouy system by wave motion emulation modelling,Sustainable Energy Technologies and Assessments, Volume 43, 100962, ISSN 2213-1388, https://doi.org/10.1016/j.seta.2020.100962.

[14] Kristof L. De Koker, Guillaume Crevecoeur, Bart Meersman, Marc Vantorre and Lieven Vandevelde (2017) A wave emulator for ocean wave energy, a Froude-scaled dry power take-off test setup, Renewable Energy, Volume 105, Pages 712-721, ISSN 0960-1481, https://doi.org/10.1016/j.renene.2016.12.080.

[15] Eriksson M, Isberg J and Leijon M (2005) Hydrodynamic modelling of a direct drive wave energy converter. International Journal of Engineering Science 43, 1377-1387.